Linear power corrections to top quark production processes

Melih A. Ozcelik

IJCLab, CNRS, Université Paris-Saclay

melih.ozcelik@ijclab.in2p3.fr

based on JHEP05(2023)153, JHEP01(2024)074
with **S. Makarov**, **K. Melnikov**, **P. Nason**

DIS 2024, Grenoble,
10 April 2024

Part I

Introduction:
Renormalons & Power Corrections

precision at colliders

- improved experimental precision at colliders

precision at colliders

- improved experimental precision at colliders
- in order to detect potential deviations from SM, require precise theory predictions

precision at colliders

- improved experimental precision at colliders
- in order to detect potential deviations from SM, require precise theory predictions
- determination of SM parameters: top mass m_t, strong coupling α_s etc.

precision at colliders

- improved experimental precision at colliders
- in order to detect potential deviations from SM, require precise theory predictions
- determination of SM parameters: top mass m_t, strong coupling α_s etc.

- *master equation* for hadron colliders:

$$d\sigma = \sum_{i,j} \int dx_1 dx_2 \, f_{i/p}(x_1) \, f_{j/p}(x_2) \, d\hat{\sigma}_{ij}(x_1 P_1, x_2 P_2) \tag{1}$$

  - $f_{i/p}$: parton distribution function (PDF)
  - $d\hat{\sigma}_{ij}$: partonic cross-section

cross-sections: QCD corrections

$$d\sigma = \sum_{i,j} \int dx_1 dx_2 \, f_{i/p}(x_1) \, f_{j/p}(x_2) \, d\hat{\sigma}_{ij}(x_1 P_1, x_2 P_2) \tag{2}$$

- partonic cross-section can be represented by Feynman diagrams

cross-sections: QCD corrections

$$d\sigma = \sum_{i,j} \int dx_1 dx_2 \, f_{i/p}(x_1) \, f_{j/p}(x_2) \, d\hat{\sigma}_{ij}(x_1 P_1, x_2 P_2) \tag{2}$$

- partonic cross-section can be represented by Feynman diagrams
- for precision studies, require higher-order perturbative QCD corrections

cross-sections: QCD corrections

$$d\sigma = \sum_{i,j} \int dx_1 dx_2 \, f_{i/p}(x_1) \, f_{j/p}(x_2) \, d\hat{\sigma}_{ij}(x_1 P_1, x_2 P_2) \tag{2}$$

- partonic cross-section can be represented by Feynman diagrams
- for precision studies, require higher-order perturbative QCD corrections

$$d\sigma = d\sigma_{\text{LO}} + \left(\frac{\alpha_s}{\pi}\right) d\sigma_{\text{NLO}} + \left(\frac{\alpha_s}{\pi}\right)^2 d\sigma_{\text{NNLO}} + \left(\frac{\alpha_s}{\pi}\right)^3 d\sigma_{\text{N}^3\text{LO}} + \ldots$$

cross-sections: QCD corrections

$$d\sigma = \sum_{i,j} \int dx_1 dx_2 \, f_{i/p}(x_1) \, f_{j/p}(x_2) \, d\hat{\sigma}_{ij}(x_1 P_1, x_2 P_2) \tag{2}$$

- partonic cross-section can be represented by Feynman diagrams
- for precision studies, require higher-order perturbative QCD corrections

$$d\sigma = d\sigma_{\text{LO}} + \underbrace{\left(\frac{\alpha_s}{\pi}\right) d\sigma_{\text{NLO}}}_{10\%} + \underbrace{\left(\frac{\alpha_s}{\pi}\right)^2 d\sigma_{\text{NNLO}}}_{1\%} + \underbrace{\left(\frac{\alpha_s}{\pi}\right)^3 d\sigma_{\text{N}^3\text{LO}}}_{0.1\%} + \ldots$$

cross-sections: QCD corrections

$$d\sigma = \sum_{i,j} \int dx_1 dx_2 \, f_{i/p}(x_1) \, f_{j/p}(x_2) \, d\hat{\sigma}_{ij}(x_1 P_1, x_2 P_2) \tag{2}$$

- partonic cross-section can be represented by Feynman diagrams
- for precision studies, require higher-order perturbative QCD corrections

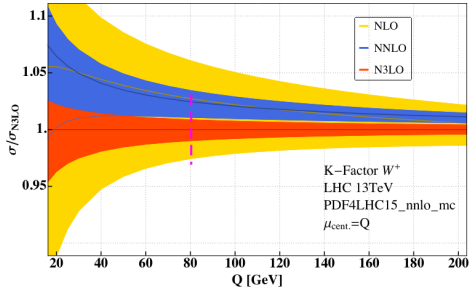

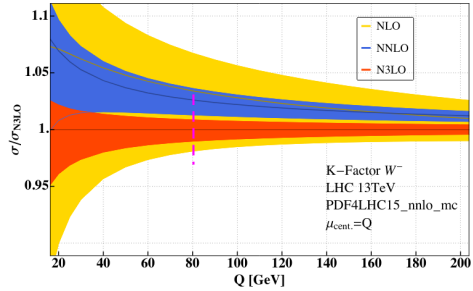

Drell-Yan N^{3}LO $\sim 1\%$ correction

[Duhr, Dulat, Mistlberger; JHEP 11 (2020) 143]

cross-sections: QCD corrections

$$d\sigma = \sum_{i,j} \int dx_1 dx_2 \, f_{i/p}(x_1) \, f_{j/p}(x_2) \, d\hat{\sigma}_{ij}(x_1 P_1, x_2 P_2) \tag{2}$$

- partonic cross-section can be represented by Feynman diagrams
- for precision studies, require higher-order perturbative QCD corrections

$$d\sigma = d\sigma_{\text{LO}} + \underbrace{\left(\frac{\alpha_s}{\pi}\right) d\sigma_{\text{NLO}}}_{10\%} + \underbrace{\left(\frac{\alpha_s}{\pi}\right)^2 d\sigma_{\text{NNLO}}}_{1\%} + \underbrace{\left(\frac{\alpha_s}{\pi}\right)^3 d\sigma_{\text{N}^3\text{LO}}}_{0.1\%} + \ldots$$
$$+ \left(\frac{\Lambda_{\text{QCD}}}{Q}\right) d\sigma^{\text{NP}}_{\text{linear}} + \ldots$$

cross-sections: QCD corrections

$$d\sigma = \sum_{i,j} \int dx_1 dx_2 \, f_{i/p}(x_1) \, f_{j/p}(x_2) \, d\hat{\sigma}_{ij}(x_1 P_1, x_2 P_2) \tag{2}$$

- partonic cross-section can be represented by Feynman diagrams
- for precision studies, require higher-order perturbative QCD corrections

$$d\sigma = d\sigma_{\text{LO}} + \underbrace{\left(\frac{\alpha_s}{\pi}\right) d\sigma_{\text{NLO}}}_{10\%} + \underbrace{\left(\frac{\alpha_s}{\pi}\right)^2 d\sigma_{\text{NNLO}}}_{1\%} + \underbrace{\left(\frac{\alpha_s}{\pi}\right)^3 d\sigma_{\text{N}^3\text{LO}}}_{0.1\%} + \ldots$$

$$+ \left(\frac{\Lambda_{\text{QCD}}}{Q}\right) d\sigma^{\text{NP}}_{\text{linear}} + \ldots \qquad \text{with } \Lambda_{\text{QCD}} \sim 300 \text{ MeV}, \; Q \sim 30 - 100 \text{ GeV}$$

cross-sections: QCD corrections

$$d\sigma = \sum_{i,j} \int dx_1 dx_2 \, f_{i/p}(x_1) \, f_{j/p}(x_2) \, d\hat{\sigma}_{ij}(x_1 P_1, x_2 P_2) \tag{2}$$

- partonic cross-section can be represented by Feynman diagrams
- for precision studies, require higher-order perturbative QCD corrections

$$d\sigma = d\sigma_{\text{LO}} + \underbrace{\left(\frac{\alpha_s}{\pi}\right) d\sigma_{\text{NLO}}}_{10\%} + \underbrace{\left(\frac{\alpha_s}{\pi}\right)^2 d\sigma_{\text{NNLO}}}_{1\%} + \underbrace{\left(\frac{\alpha_s}{\pi}\right)^3 d\sigma_{\text{N}^3\text{LO}}}_{0.1\%} + \ldots$$

$$+ \underbrace{\left(\frac{\Lambda_{\text{QCD}}}{Q}\right) d\sigma^{\text{NP}}_{\text{linear}}}_{0.1\%-1\%} + \ldots \qquad \text{with } \Lambda_{\text{QCD}} \sim 300 \text{ MeV}, \; Q \sim 30 - 100 \text{ GeV}$$

cross-sections: QCD corrections

$$d\sigma = \sum_{i,j} \int dx_1 dx_2 \, f_{i/p}(x_1) \, f_{j/p}(x_2) \, d\hat{\sigma}_{ij}(x_1 P_1, x_2 P_2) \tag{2}$$

- partonic cross-section can be represented by Feynman diagrams
- for precision studies, require higher-order perturbative QCD corrections

$$d\sigma = d\sigma_{\text{LO}} + \underbrace{\left(\frac{\alpha_s}{\pi}\right) d\sigma_{\text{NLO}}}_{10\%} + \underbrace{\left(\frac{\alpha_s}{\pi}\right)^2 d\sigma_{\text{NNLO}}}_{1\%} + \underbrace{\left(\frac{\alpha_s}{\pi}\right)^3 d\sigma_{\text{N}^3\text{LO}}}_{0.1\%} + \ldots$$

$$+ \underbrace{\left(\frac{\Lambda_{\text{QCD}}}{Q}\right) d\sigma^{\text{NP}}_{\text{linear}}}_{0.1\%-1\%} + \ldots \qquad \text{with } \Lambda_{\text{QCD}} \sim 300 \text{ MeV}, \; Q \sim 30 - 100 \text{ GeV}$$

$\rightarrow$ **non-perturbative corrections may become relevant!**

linear power corrections: renormalon calculus

- power corrections can be computed by considering perturbative corrections with massive gluon of mass λ

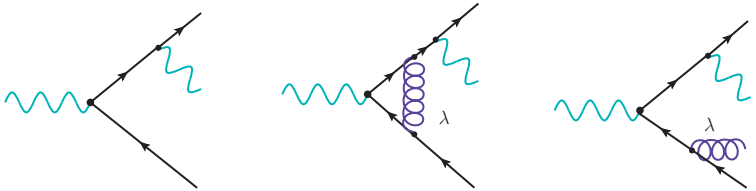

linear power corrections: renormalon calculus

- power corrections can be computed by considering perturbative corrections with massive gluon of mass λ

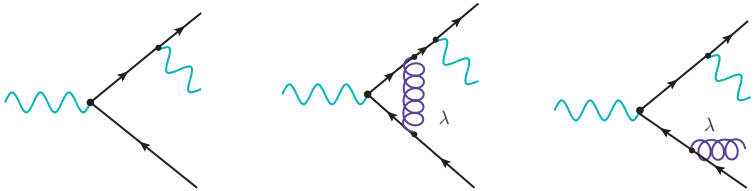

- direct relation between $\lambda^p \to \Lambda^p_{\rm QCD}$

linear power corrections: renormalon calculus

- power corrections can be computed by considering perturbative corrections with massive gluon of mass λ

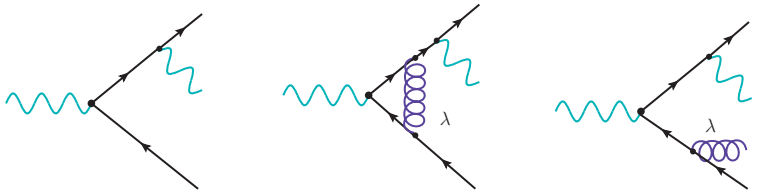

- direct relation between $\lambda^p \to \Lambda^p_{\rm QCD}$
- for phenomenological applications only linear terms λ/Q are relevant, higher orders in λ are surpressed by $\mathcal{O}(\Lambda^2_{\rm QCD}/Q^2)$

non-perturbative physics

In order to compute linear power corrections with renormalon calculus,

- compute NLO corrections with a massive gluon of mass λ
- can be applied only to processes with no gluons in the Born process

Recent progresses with renormalon calculus,

- linear power corrections to event shape variables $\rightarrow$ can be used for α_s extraction
  [F. Caola, S. Ferrario Ravasio, G. Limatola, K. Melnikov, P. Nason, M.A. Ozcelik, JHEP 12 (2022) 062]
- linear power corrections to top quark processes at the LHC $\rightarrow$ may be used for m_t extract.
  [S. Makarov, K. Melnikov, P. Nason, M.A. Ozcelik, JHEP 05 (2023) 153 & JHEP 01 (2024) 074]

Top mass determination

- most precise top mass measurements at LHC come from "direct measurements"
  - → kinematic reconstruction of measured top quark decay products
- currently, typical error quoted to be around $\Delta m_t \sim 500$ MeV
  - → future (HL-LHC), envisaged uncertainty $\Delta m_t \sim 200$ MeV
- direct measurements → measured top quark mass is the value of the top mass parameter in the Monte Carlo generator

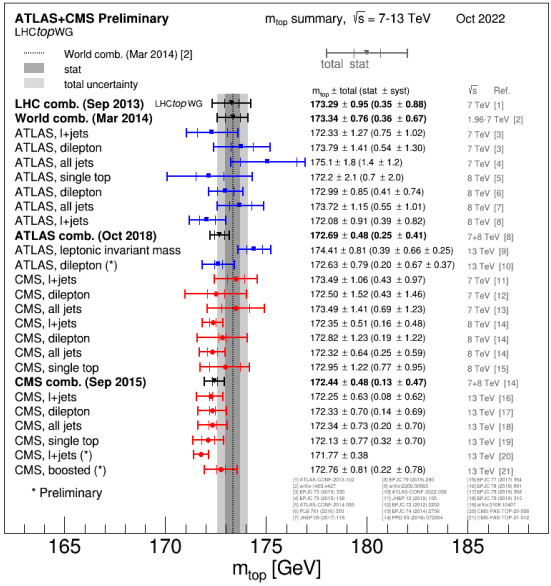

Top mass determination: scheme dependence

- top quark mass parameter requires renormalisation

Top mass determination: scheme dependence

- top quark mass parameter requires renormalisation
  $\rightarrow$ depends on renormalisation scheme

Top mass determination: scheme dependence

- top quark mass parameter requires renormalisation
  $\rightarrow$ depends on renormalisation scheme
- difference in top mass in different schemes $(A,\ B)$ $\qquad R = [1\ \text{GeV}, m_t]$

$$m_t^A - m_t^B \sim \underbrace{R\alpha_s(R)}_{\text{MeV}-\text{GeV}} \tag{3}$$

Top mass determination: scheme dependence

- top quark mass parameter requires renormalisation
  $\rightarrow$ depends on renormalisation scheme
- difference in top mass in different schemes $(A,\ B)$ $\qquad R = [1\ \text{GeV}, m_t]$

$$m_t^A - m_t^B \sim \underbrace{R\alpha_s(R)}_{\text{MeV}-\text{GeV}} \tag{3}$$

- experimental result must specify the scheme

Top mass determination: scheme dependence

- top quark mass parameter requires renormalisation
  $\rightarrow$ depends on renormalisation scheme
- difference in top mass in different schemes $(A,\ B)$ $\qquad R = [1\ \text{GeV}, m_t]$

$$m_t^A - m_t^B \sim \underbrace{R\alpha_s(R)}_{\text{MeV}-\text{GeV}} \tag{3}$$

- experimental result must specify the scheme
  - pole mass scheme

Top mass determination: scheme dependence

- top quark mass parameter requires renormalisation
  $\rightarrow$ depends on renormalisation scheme
- difference in top mass in different schemes $(A,\ B)$ $\qquad R = [1\ \text{GeV}, m_t]$

$$m_t^A - m_t^B \sim \underbrace{R\alpha_s(R)}_{\text{MeV}-\text{GeV}} \tag{3}$$

- experimental result must specify the scheme
  - pole mass scheme
  - $\overline{\text{MS}}$-scheme
  - ...

Top mass determination: scheme dependence

- top quark mass parameter requires renormalisation
  $\rightarrow$ depends on renormalisation scheme
- difference in top mass in different schemes $(A,\ B)$ $\qquad R = [1\ \text{GeV}, m_t]$

$$m_t^A - m_t^B \sim \underbrace{R\alpha_s(R)}_{\text{MeV}-\text{GeV}} \tag{3}$$

- experimental result must specify the scheme
  - pole mass scheme
  - $\overline{\text{MS}}$-scheme
  - ...
- the pole mass scheme suffers from renormalon ambiguity Λ_{QCD}/m_t

Top mass determination: scheme dependence

- top quark mass parameter requires renormalisation
  $\rightarrow$ depends on renormalisation scheme
- difference in top mass in different schemes $(A,\ B)$ $\qquad R = [1\ \text{GeV}, m_t]$

$$m_t^A - m_t^B \sim \underbrace{R\alpha_s(R)}_{\text{MeV}-\text{GeV}} \tag{3}$$

- experimental result must specify the scheme
  - pole mass scheme
  - $\overline{\text{MS}}$-scheme
  - ...
- the pole mass scheme suffers from renormalon ambiguity Λ_{QCD}/m_t
- short-distance mass schemes ($\overline{\text{MS}}$, ...) are free from this issue

Top mass determination: scheme dependence

- top quark mass parameter requires renormalisation
  $\rightarrow$ depends on renormalisation scheme
- difference in top mass in different schemes $(A,\ B)$ $\qquad R = [1\ \text{GeV}, m_t]$

$$m_t^A - m_t^B \sim \underbrace{R\alpha_s(R)}_{\text{MeV}-\text{GeV}} \tag{3}$$

- experimental result must specify the scheme
  - pole mass scheme
  - $\overline{\text{MS}}$-scheme
  - ...
- the pole mass scheme suffers from renormalon ambiguity Λ_{QCD}/m_t
- short-distance mass schemes ($\overline{\text{MS}}$, ...) are free from this issue

$\rightarrow$ investigate mass scheme-dependence on linear power corrections to top quark production cross-sections and observables

Part II

Linear power corrections to top quark processes

[S. Makarov, K. Melnikov, P. Nason, M.A. Ozcelik, JHEP 05 (2023) 153 & JHEP 01 (2024) 074]

Massive case: presence or absence of linear power correction

For processes with *massive* quarks:

- single top production,
- $t\bar{t}$ production,
- ...

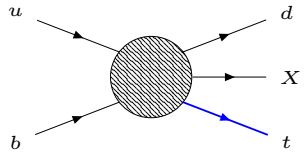

we can make the following statements on presence or absence of linear power corrections:

[Makarov, Melnikov, Nason, Ozcelik, JHEP 05 (2023) 153]

- *virtual* corrections **do** induce linear corrections
  - in the soft limit at next-to-soft approximation
- *real* corrections **do** induce linear corrections
  - in the soft limit at *next-to-soft* approximation
- need amplitudes at *next-to-soft* approximation
  $\rightarrow$ can use *Low-Burnett-Kroll* theorem

Real radiation: Low-Burnett-Kroll theorem

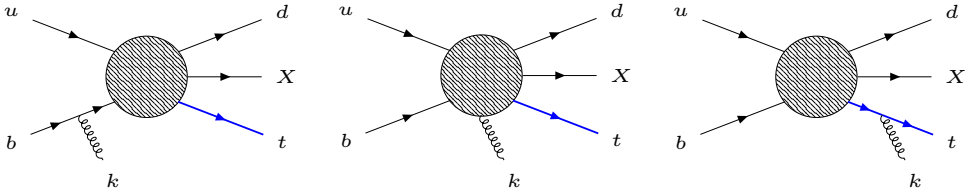

Real radiation: Low-Burnett-Kroll theorem

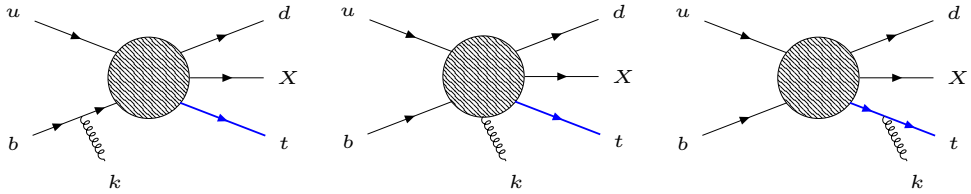

- the reduced real radiation amplitude $\mathcal{M}^\mu$ reads:

$$\mathcal{M}^\mu = \bar{u}(q_t)\gamma^\mu \frac{\not{q}_t + \not{k} + m_t}{d_t} \mathrm{N}(q_t + k, p_b, q_d, ...)u(p_b) + \bar{u}(q_t)\mathrm{N}(q_t, p_b - k, q_d, ...)\frac{\not{p}_b - \not{k}}{d_b}\gamma^\mu u(p_b) + \mathcal{M}^\mu_{\mathrm{reg}}(q_t, p_b, q_d, ..|k), \tag{4}$$

Real radiation: Low-Burnett-Kroll theorem

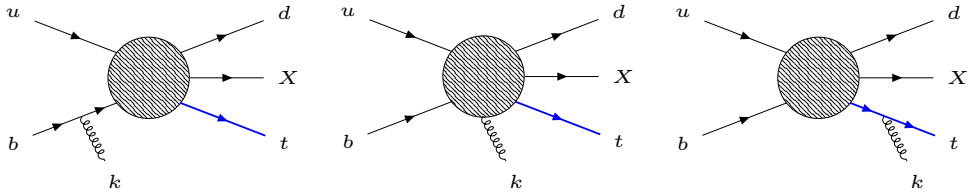

- the reduced real radiation amplitude $\mathcal{M}^\mu$ reads:

$$\mathcal{M}^\mu = \bar{u}(q_t)\gamma^\mu \frac{\not{q}_t + \not{k} + m_t}{d_t} \mathrm{N}(q_t + k, p_b, q_d, ...)u(p_b) + \bar{u}(q_t)\mathrm{N}(q_t, p_b - k, q_d, ...)\frac{\not{p}_b - \not{k}}{d_b}\gamma^\mu u(p_b) + \mathcal{M}^\mu_{\mathrm{reg}}(q_t, p_b, q_d, ..|k), \tag{4}$$

- need $\mathcal{M}^\mu_{\mathrm{reg}}$ up to sub-leading term within $\mathcal{M}$

Real radiation: Low-Burnett-Kroll theorem

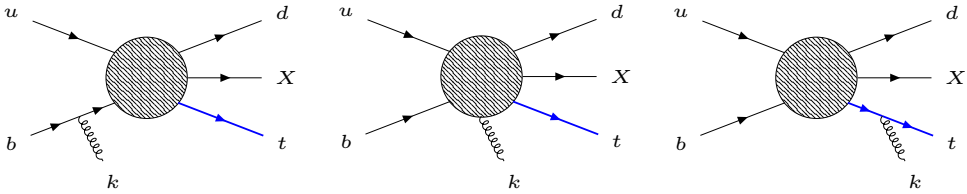

- use condition: $k_\mu \mathcal{M}^\mu = 0$

Real radiation: Low-Burnett-Kroll theorem

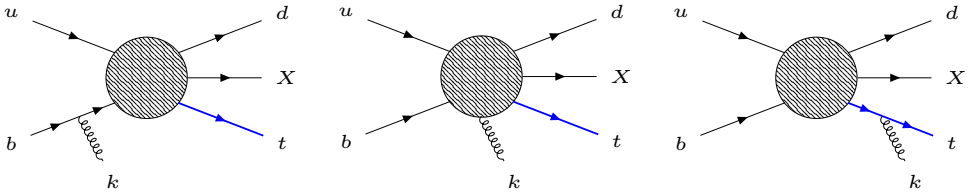

- use condition: $k_\mu \mathcal{M}^\mu = 0$

$$\mathcal{M}^\mu_{\rm reg}(q_t, p_b, q_d, ...|k=0) = -\bar{u}_t \left[\frac{\partial \mathrm{N}(q_t, p_b, q_d, ...)}{\partial q_{t,\mu}} + \frac{\partial \mathrm{N}(q_t, p_b, q_d, ...)}{\partial p_{b,\mu}} \right] u_b. \qquad (4)$$

Real radiation: Low-Burnett-Kroll theorem

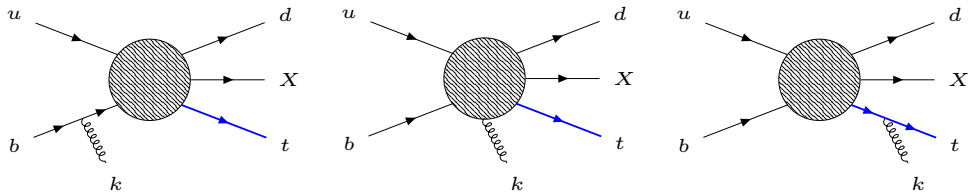

- use condition: $k_\mu \mathcal{M}^\mu = 0$

$$\mathcal{M}^\mu_{\text{reg}}(q_t, p_b, q_d, ...|k=0) = -\bar{u}_t \left[\frac{\partial \mathrm{N}(q_t, p_b, q_d, ...)}{\partial q_{t,\mu}} + \frac{\partial \mathrm{N}(q_t, p_b, q_d, ...)}{\partial p_{b,\mu}} \right] u_b. \quad (4)$$

- we now have all the ingredients
  $\rightarrow$ construct $|\mathcal{M}|^2$ up to *next-to-soft* approximation

Real radiation: Low-Burnett-Kroll theorem

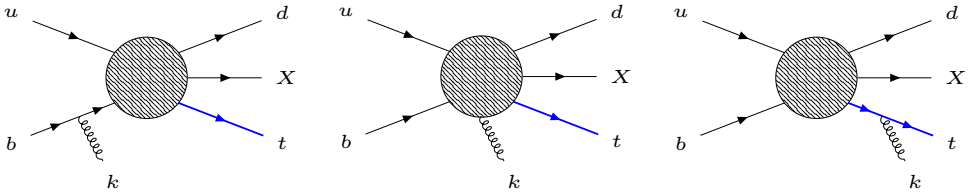

- we obtain

$$|\mathcal{M}|^2 = -J^\mu J_\mu F_{\rm LO}(q_t, p_b, q_d, ...) - J_\mu L^\mu F_{\rm LO}(q_t, p_b, q_d, ...). \tag{4}$$

Real radiation: Low-Burnett-Kroll theorem

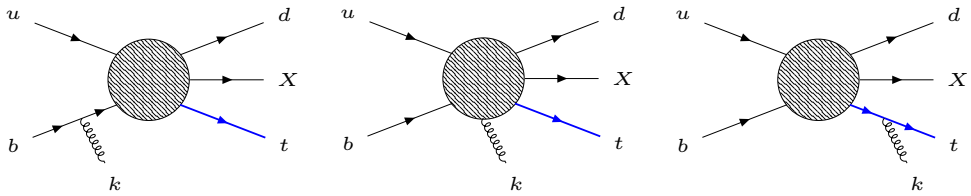

- we obtain

$$|\mathcal{M}|^2 = -J^\mu J_\mu F_{\rm LO}(q_t, p_b, q_d, ...) - J_\mu L^\mu F_{\rm LO}(q_t, p_b, q_d, ...). \tag{4}$$

$$J^\mu = J_t^\mu + J_b^\mu, \quad L^\mu = L_t^\mu - L_b^\mu, \quad J_t^\mu = \frac{2q_t + k^\mu}{d_t}, \quad J_b^\mu = \frac{2p_b^\mu - k^\mu}{d_b},$$
$$L_t^\mu = J_t^\mu k^\nu \frac{\partial}{\partial q_t^\nu} - \frac{\partial}{\partial q_{t,\mu}}, \quad L_b^\mu = J_b^\mu k^\nu \frac{\partial}{\partial p_b^\nu} + \frac{\partial}{\partial p_{b,\mu}}$$

Real radiation: Low-Burnett-Kroll theorem

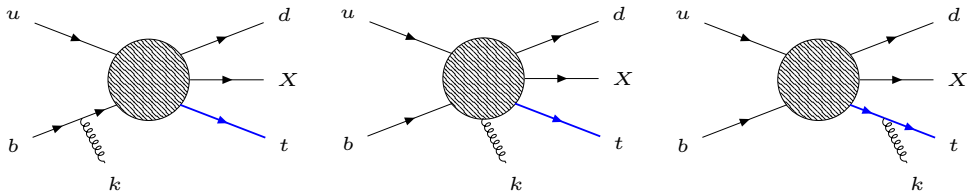

- we obtain

$$|\mathcal{M}|^2 = -J^\mu J_\mu F_{\rm LO}(q_t, p_b, q_d, ...) - J_\mu L^\mu F_{\rm LO}(q_t, p_b, q_d, ...). \tag{4}$$

- $|\mathcal{M}|^2$ in the next-to-soft approximation can be related to the leading-order $F_{\rm LO}$ in a *process-independent* manner

Real radiation: phase-space integration

- real emission contribution involves phase-space dLips($p_u, p_b; q_d, q_t, p_X, k$) with emitted gluon

Real radiation: phase-space integration

- real emission contribution involves phase-space dLips$(p_u, p_b; q_d, q_t, p_X, k)$ with emitted gluon
  $\rightarrow$ need to relate to LO phase-space dLips$(p_u, p_b; p_d, p_t, p_X)$

Real radiation: phase-space integration

- real emission contribution involves phase-space dLips$(p_u, p_b; q_d, q_t, p_X, k)$ with emitted gluon
  $\rightarrow$ need to relate to LO phase-space dLips$(p_u, p_b; p_d, p_t, p_X)$

- perform momentum mapping:

$$q_t = p_t - k + \frac{p_t k}{p_t p_d} p_d, \qquad q_d = p_d - \frac{p_t k}{p_t p_d} p_d \tag{5}$$

$$q_t + q_d + k + p_X = p_t + p_d + p_X \tag{6}$$

Real radiation: phase-space integration

- real emission contribution involves phase-space $\mathrm{dLips}(p_u, p_b; q_d, q_t, p_X, k)$ with emitted gluon
  $\rightarrow$ need to relate to LO phase-space $\mathrm{dLips}(p_u, p_b; p_d, p_t, p_X)$

- perform momentum mapping:

$$q_t = p_t - k + \frac{p_t k}{p_t p_d} p_d, \qquad q_d = p_d - \frac{p_t k}{p_t p_d} p_d \tag{5}$$

$$q_t + q_d + k + p_X = p_t + p_d + p_X \tag{6}$$

- can now write

$$\begin{aligned} \mathrm{dLips}(p_u, p_b; q_d, q_t, p_X, k) =& \mathrm{dLips}(p_u, p_b; p_d, p_t, p_X) \frac{d^4 k}{(2\pi)^3} \delta_+(k^2 - \lambda^2) \times \\ & \times \left[1 + \frac{p_d k}{p_t p_d} - \frac{p_t k}{p_t p_d}\right] + \mathcal{O}(\lambda^2) \end{aligned} \tag{7}$$

Virtual corrections: Low-Burnett-Kroll theorem

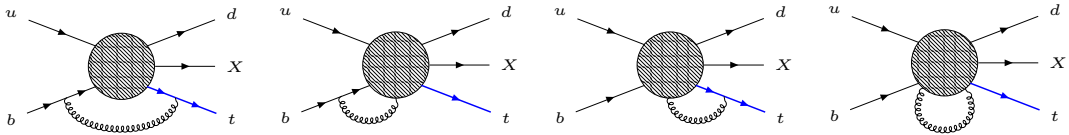

Virtual corrections: Low-Burnett-Kroll theorem

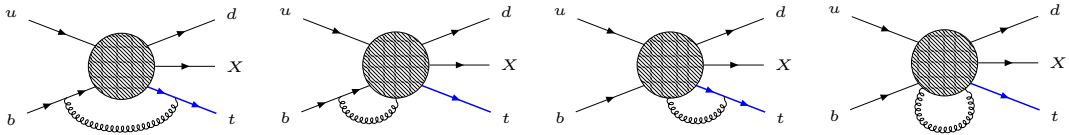

- can proceed in similar fashion as before and obtain

Virtual corrections: Low-Burnett-Kroll theorem

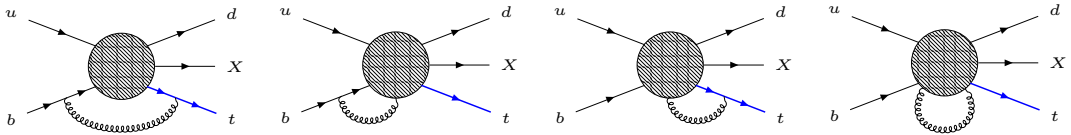

- can proceed in similar fashion as before and obtain

$$\delta[\mathcal{M}\mathcal{M}^{+}]_{\text{virt}} = \int \frac{\mathrm{d}^4 k}{(2\pi)^4} \frac{-i}{k^2-\lambda^2} \Bigg[2J_t^{\alpha} J_{b,\alpha} F_{\text{LO}} + J_t^{\alpha} J_{b,\alpha} k^{\mu}\, D_{p,\mu} F_{\text{LO}} - (J_t^{\alpha} + J_b^{\alpha}) D_{p,\alpha} F_{\text{LO}}$$

$$+ J_t^{\alpha} \text{Tr}\left[(D_{p,\alpha} \not{p}_t) \text{N} \not{p}_b \bar{\text{N}} \right] + J_b^{\alpha} \text{Tr}\left[(\not{p}_t + m_t) \text{N} (D_{p,\alpha} \not{p}_b) \bar{\text{N}} \right] \Bigg]. \tag{8}$$

$$D_p^{\mu} = \frac{\partial}{\partial p_{t,\mu}} + \frac{\partial}{\partial p_{b,\mu}}$$

Real & virtual contributions

- we can now integrate out gluon momentum and obtain for the real and virtual contributions:

$$\mathcal{T}_\lambda[\sigma_{\rm R}] = \frac{\alpha_s C_F}{2\pi}\frac{\pi\lambda}{m_t}\int \mathrm{dLips}_{\rm LO}\Bigg[\left(\frac{3}{2}-\frac{m_t^2}{p_d p_t}-\frac{m_t^2}{p_t p_b}\right) - \frac{m_t^2}{p_d p_t}p_d^\mu\left(\frac{\partial}{\partial p_d^\mu}-\frac{\partial}{\partial p_t^\mu}\right) - \frac{m_t^2}{p_t p_b}p_b^\mu\left(\frac{\partial}{\partial p_b^\mu}+\frac{\partial}{\partial p_t^\mu}\right)\Bigg] F_{\rm LO}. \tag{9}$$

$$\mathcal{T}_\lambda[\sigma_V] = -\frac{\alpha_s C_F}{2\pi}\frac{\pi\lambda}{m_t}\int \mathrm{dLips}_{\rm LO}\Bigg[\mathrm{Tr}\left[\not{p}_t \mathrm{N}\not{p}_b\bar{\mathrm{N}}\right] + \left(\frac{2p_t p_b - m_t^2}{p_t p_b} - \frac{m_t^2}{p_t p_b}p_b^\mu\left(\frac{\partial}{\partial p_b^\mu}+\frac{\partial}{\partial p_t^\mu}\right)\right)F_{\rm LO}\Bigg], \tag{10}$$

Renormalisation contribution

- we need to renormalise the heavy-quark wavefunction and mass in the on-shell scheme:

$$
\begin{aligned}
Z_m =& 1 + \frac{C_F g_s^2 m_t^{-2\epsilon} \Gamma(1+\epsilon)}{(4\pi)^{d/2}} \left[-\frac{3}{\epsilon} - 4 + \frac{2\pi\lambda}{m_t} + \mathcal{O}\left(\frac{\lambda^2}{m_t^2}\right) \right], \\
Z_2 =& 1 + \frac{C_F g_s^2 m_t^{-2\epsilon} \Gamma(1+\epsilon)}{(4\pi)^{d/2}} \left[-\frac{1}{\epsilon} - 4 + 4 \ln \frac{m_t}{\lambda} + \frac{3\lambda\pi}{m_t} + \mathcal{O}\left(\frac{\lambda^2}{m_t^2}\right) \right].
\end{aligned}
\tag{11}
$$

Renormalisation contribution

- we need to renormalise the heavy-quark wavefunction and mass in the on-shell scheme:

$$
\begin{aligned}
Z_m =& 1 + \frac{C_F g_s^2 m_t^{-2\epsilon}\Gamma(1+\epsilon)}{(4\pi)^{d/2}}\left[-\frac{3}{\epsilon} - 4 + \frac{2\pi\lambda}{m_t} + \mathcal{O}\left(\frac{\lambda^2}{m_t^2}\right)\right], \\
Z_2 =& 1 + \frac{C_F g_s^2 m_t^{-2\epsilon}\Gamma(1+\epsilon)}{(4\pi)^{d/2}}\left[-\frac{1}{\epsilon} - 4 + 4\ln\frac{m_t}{\lambda} + \frac{3\lambda\pi}{m_t} + \mathcal{O}\left(\frac{\lambda^2}{m_t^2}\right)\right].
\end{aligned}
\tag{11}
$$

- the renormalisation contribution reads

$$
\begin{aligned}
\mathcal{T}_\lambda\left[\sigma_{\rm ren}\right] = \frac{\alpha_s C_F}{2\pi}\frac{\pi\lambda}{m_t}\int \mathrm{dLips}_{\rm LO}\Bigg[&\frac{3}{2}F_{\rm LO} + m_t \mathrm{Tr}\left[(\not{p}_t + m_t)\frac{\partial \mathrm{N}}{\partial m_t}\not{p}_b \bar{\mathrm{N}}\right] \\
&+ m_t \mathrm{Tr}\left[(\not{p}_t + m_t)\mathrm{N}\not{p}_b\frac{\partial \bar{\mathrm{N}}}{\partial m_t}\right]\Bigg].
\end{aligned}
\tag{12}
$$

Top quark mass scheme redefinition

- we now perform a mass scheme redefinition from pole-mass scheme to short-distance mass scheme

$$m_t = \tilde{m}_t \left(1 - \frac{C_F \alpha_s}{2\pi} \frac{\pi \lambda}{m_t}\right). \tag{13}$$

Top quark mass scheme redefinition

- we now perform a mass scheme redefinition from pole-mass scheme to short-distance mass scheme

$$m_t = \tilde{m}_t \left(1 - \frac{C_F \alpha_s}{2\pi} \frac{\pi\lambda}{m_t}\right). \tag{13}$$

- need to account for both explicit (m_t) and implicit (p_t) mass change

Top quark mass scheme redefinition

- we now perform a mass scheme redefinition from pole-mass scheme to short-distance mass scheme

$$m_t = \tilde{m}_t \left(1 - \frac{C_F \alpha_s}{2\pi} \frac{\pi \lambda}{m_t}\right). \tag{13}$$

- need to account for both explicit (m_t) and implicit (p_t) mass change
  $\rightarrow$ can be done in a *process-independent* manner

Top quark mass scheme redefinition

- we now perform a mass scheme redefinition from pole-mass scheme to short-distance mass scheme

$$m_t = \tilde{m}_t \left(1 - \frac{C_F \alpha_s}{2\pi} \frac{\pi\lambda}{m_t}\right). \tag{13}$$

- need to account for both explicit (m_t) and implicit (p_t) mass change
  $\rightarrow$ can be done in a *process-independent* manner

$$\begin{aligned}\sigma_{\rm LO}(m_t) - \sigma_{\rm LO}(\tilde{m}_t) = \delta\sigma^{\rm expl}_{\rm mass} + \delta\sigma^{\rm impl}_{\rm mass} = \frac{C_F\alpha_s}{2\pi}\frac{\pi\lambda}{m_t}\int {\rm dLips}_{\rm LO}\times \\ \times\left[\frac{m_t^2}{p_d p_t}\left[1 + p_d^\mu\left(\frac{\partial}{\partial p_d^\mu} - \frac{\partial}{\partial p_t^\mu}\right)\right] F_{\rm LO} - m_t {\rm Tr}\left[1{\rm N}\not{p}_b\bar{\rm N}\right]\right. \\ \left. - m_t {\rm Tr}\left[(\not{p}_t + m_t)\left(\frac{\partial {\rm N}}{\partial m_t}\not{p}_b\bar{\rm N} + {\rm N}\not{p}_b\frac{\partial\bar{\rm N}}{\partial m_t}\right)\right]\right].\end{aligned} \tag{14}$$

Combined contributions

- combining all contributions, we obtain in the short-distance mass scheme:

$$\delta\sigma_{\rm NLO} = \sigma_R + \sigma_V + \sigma_{\rm ren} + \delta\sigma^{\rm expl}_{\rm mass} + \delta\sigma^{\rm impl}_{\rm mass} \tag{15}$$

Combined contributions

- combining all contributions, we obtain in the short-distance mass scheme:

$$\delta\sigma_{\rm NLO} = \sigma_R + \sigma_V + \sigma_{\rm ren} + \delta\sigma^{\rm expl}_{\rm mass} + \delta\sigma^{\rm impl}_{\rm mass} \tag{15}$$

$$\mathcal{T}_\lambda\left[\delta\sigma_{\rm NLO}\right] = \frac{\alpha_s C_F}{2\pi}\frac{\pi\lambda}{m_t}\int {\rm dLips_{LO}}\,\left(F_{\rm LO} - {\rm Tr}\left[\not{p}_t \mathsf{N} \not{p}_b \bar{\mathsf{N}}\right] - m_t {\rm Tr}\left[1\mathsf{N}\not{p}_b\bar{\mathsf{N}}\right]\right) = 0. \tag{16}$$

Combined contributions

- combining all contributions, we obtain in the short-distance mass scheme:

$$\delta\sigma_{\rm NLO} = \sigma_R + \sigma_V + \sigma_{\rm ren} + \delta\sigma^{\rm expl}_{\rm mass} + \delta\sigma^{\rm impl}_{\rm mass} \tag{15}$$

$$\mathcal{T}_\lambda\left[\delta\sigma_{\rm NLO}\right] = \frac{\alpha_s C_F}{2\pi}\frac{\pi\lambda}{m_t}\int {\rm dLips}_{\rm LO}\,\left(F_{\rm LO} - {\rm Tr}\left[\not{p}_t \mathrm{N} \not{p}_b \bar{\mathrm{N}}\right] - m_t {\rm Tr}\left[1\mathrm{N}\not{p}_b\bar{\mathrm{N}}\right]\right) = 0. \tag{16}$$

- for total cross-sections, there are **no linear power corrections** for single-top production type processes within the short-distance mass scheme

Combined contributions

- combining all contributions, we obtain in the short-distance mass scheme:

$$\delta\sigma_{\rm NLO} = \sigma_R + \sigma_V + \sigma_{\rm ren} + \delta\sigma^{\rm expl}_{\rm mass} + \delta\sigma^{\rm impl}_{\rm mass} \tag{15}$$

$$\mathcal{T}_\lambda\left[\delta\sigma_{\rm NLO}\right] = \frac{\alpha_s C_F}{2\pi}\frac{\pi\lambda}{m_t}\int {\rm dLips}_{\rm LO}\,\left(F_{\rm LO} - {\rm Tr}\left[\not{p}_t {\rm N}\not{p}_b\bar{\rm N}\right] - m_t {\rm Tr}\left[1{\rm N}\not{p}_b\bar{\rm N}\right]\right) = 0. \tag{16}$$

- for total cross-sections, there are **no linear power corrections** for single-top production type processes within the short-distance mass scheme

- what about observables, e.g. kinematic distributions, ... ?

Kinematic observables

- observable that depends on the momentum of the top quark

$$O_X = \int \mathrm{d}\sigma \; X(q_t). \tag{17}$$

Kinematic observables

- observable that depends on the momentum of the top quark

$$O_X = \int \mathrm{d}\sigma \; X(q_t). \tag{17}$$

- new component is the expansion of q_t in X

$$X(q_t) = X(p_t) + \frac{\partial X(p_t)}{\partial p_t^\mu} \left(\frac{p_t k}{p_t p_d} p_d^\mu - k^\mu \right). \tag{18}$$

Kinematic observables

- observable that depends on the momentum of the top quark

$$O_X = \int \mathrm{d}\sigma \; X(q_t). \tag{17}$$

- new component is the expansion of q_t in X

$$X(q_t) = X(p_t) + \frac{\partial X(p_t)}{\partial p_t^\mu} \left(\frac{p_t k}{p_t p_d} p_d^\mu - k^\mu \right). \tag{18}$$

- now compute $\mathcal{T}_\lambda[O_X]$ and obtain for the observable

$$O_X = \int \mathrm{d}\sigma_{\mathrm{LO}} \left[X(p_t) + \frac{\alpha_s C_F}{2\pi} \frac{\pi\lambda}{m_t} \left(p_t^\mu - \frac{2m_t^2}{p_b p_t} p_b^\mu \right) \frac{\partial X(p_t)}{\partial p_t^\mu} \right]$$

Kinematic observables

- observable that depends on the momentum of the top quark

$$O_X = \int \mathrm{d}\sigma \; X(q_t). \tag{17}$$

- new component is the expansion of q_t in X

$$X(q_t) = X(p_t) + \frac{\partial X(p_t)}{\partial p_t^\mu} \left(\frac{p_t k}{p_t p_d} p_d^\mu - k^\mu \right). \tag{18}$$

- now compute $\mathcal{T}_\lambda[O_X]$ and obtain for the observable

$$O_X = \int \mathrm{d}\sigma_{\mathrm{LO}} \; X\left(p_t + \frac{\alpha_s C_F}{2\pi} \frac{\pi\lambda}{m_t} \left(p_t - \frac{2m_t^2}{p_b p_t} p_b \right) \right) \tag{19}$$

$\rightarrow$ the linear term can be understood as a shift in the observable

Kinematic observables

- observable that depends on the momentum of the top quark

$$O_X = \int \mathrm{d}\sigma \; X(q_t). \tag{17}$$

- new component is the expansion of q_t in X

$$X(q_t) = X(p_t) + \frac{\partial X(p_t)}{\partial p_t^\mu} \left(\frac{p_t k}{p_t p_d} p_d^\mu - k^\mu \right). \tag{18}$$

- now compute $\mathcal{T}_\lambda[O_X]$ and obtain for the observable

$$O_X = \int \mathrm{d}\sigma_{\mathrm{LO}} \; X\left(p_t + \frac{\alpha_s C_F}{2\pi} \frac{\pi\lambda}{m_t} \left(p_t - \frac{2m_t^2}{p_b p_t} p_b \right) \right) \tag{19}$$

  $\rightarrow$ the linear term can be understood as a shift in the observable

- for observables, linear power corrections **do not vanish** within the short-distance mass scheme

Top quark pair production at the Tevatron

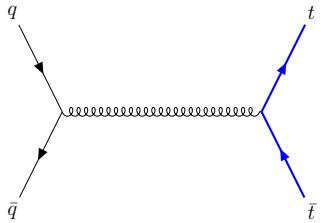

- the dominant channel for $t\bar{t}$ production at the Tevatron is via $q\bar{q}$ fusion
- tree-level diagram contains gluon but it is **off-shell**
- can generalise previous calculation to dipole pairs
- for total cross-sections, there are **no linear power corrections** for $t\bar{t}$ production type processes within the short-distance mass scheme
- for observables, linear power corrections **do not vanish** within the short-distance mass scheme

Top quark pair production at the Tevatron: $p_{t\perp}$, y_t, $s_{t\bar{t}}$

- it is now straightforward to compute the linear shift for $p_{t\perp}$, y_t and $s_{t\bar{t}}$

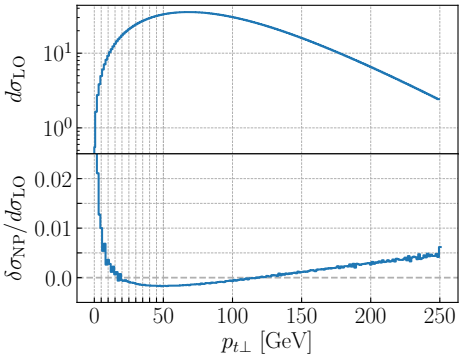

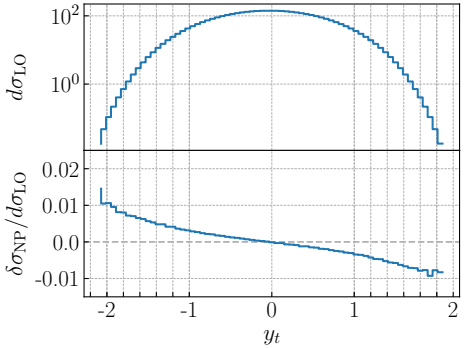

- can now compute non-perturbative shift at Tevatron ($\sqrt{s} = 1.8$ TeV)

Top quark pair production at the Tevatron: $p_{t\perp}$, y_t, $s_{t\bar{t}}$

- it is now straightforward to compute the linear shift for $p_{t\perp}$, y_t and $s_{t\bar{t}}$

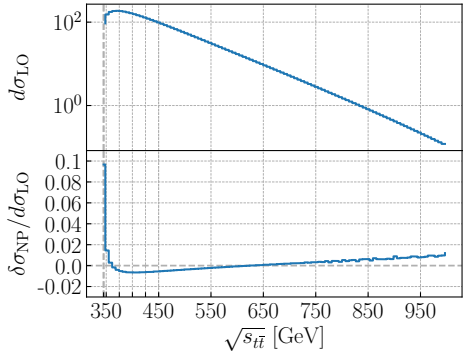

- can now compute non-perturbative shift at Tevatron ($\sqrt{s} = 1.8$ TeV)

Part III

Conclusions & Outlook

Summary

- improved understanding of analytic structure of linear power corrections
- computed linear power corrections for event-shape variables (C-parameter, thrust)
- for top quark production processes, **there are no linear power corrections** to total cross-sections within the short-distance mass scheme ($\overline{\text{MS}}$-scheme)
- however for observables ($p_{t\perp}$, y_t, $s_{t\bar{t}}$), **there are linear power corrections** within the short-distance mass scheme ($\overline{\text{MS}}$-scheme)
- computed expressions for observables, e.g. $p_{t\perp}$, y_t and $s_{t\bar{t}}$, ...
- similar results and conclusions for other (abelian) type processes ...

Thank you for attention!

Backup

non-perturbative physics: Renormalons

- Renormalon model identifies simple class of diagrams that dominate in the large n_f limit **[Beneke, Braun, Dokshitzer, Marchesini, Smye, Webber, etc.]**

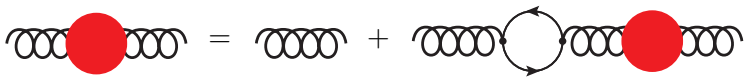

- example: 3-jet event $Z^*/\gamma^* \to q\bar{q}\gamma$

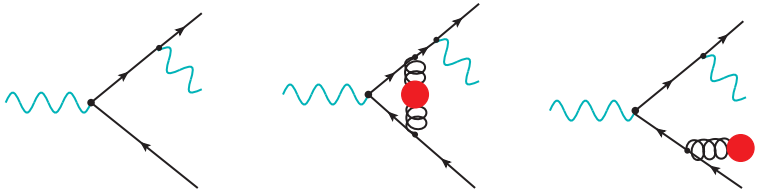

- each diagram can be computed perturbatively,

$$d\sigma = d\sigma^{(0)} + \left(\frac{\alpha_s}{\pi}\right) d\sigma^{(1)} + \left(\frac{\alpha_s}{\pi}\right)^2 n_f \, d\sigma^{(2)} + \left(\frac{\alpha_s}{\pi}\right)^3 n_f^2 \, d\sigma^{(3)} + \ldots \tag{20}$$

non-perturbative physics: Renormalons

- can resum leading-n_f contributions via integral

$$\int_0^Q dk\; k^{p-1}\alpha_s(k) = \alpha_s(Q)\, Q^p \sum_{n=0}^{\infty} \underbrace{\left(\frac{\beta_0}{2\pi}\alpha_s(Q)\right)^n \frac{1}{p^{n+1}}\, n!}_{\text{factorial growth}}, \tag{21}$$

$$\text{with} \quad \alpha_s(\mu) = \frac{1}{\frac{\beta_0}{2\pi}\log\frac{\mu}{\Lambda_{\rm QCD}}}, \quad \beta_0 = \frac{11}{3}C_A - \frac{4}{3}T_F n_f. \tag{22}$$

- series is not Borel summable, ambiguity given by

$$\int dk\; k^{p-1}\,\frac{2\pi}{\beta_0}\,\frac{\Lambda_{\rm QCD}}{k-\Lambda_{\rm QCD}} = \pm 2\pi i \frac{2\pi}{\beta_0}\Lambda_{\rm QCD}^p$$

$\rightarrow$ ambiguity removed by non-perturbative power corrections $\Lambda_{\rm QCD}^p/Q^p$

Massless case: presence or absence of linear power correction

For processes with *massless* quarks:

- three-jet events,
- ...,

one can make following statements on presence or absence of linear power corrections:

[Caola, Ferrario Ravasio, Limatola, Melnikov, Nason, JHEP 01 (2022) 093]

- *virtual* corrections **do not** induce linear corrections
- *real* corrections
  - hard region **does not** induce linear corrections
  - soft radiation at next-to-soft approximation may lead to linear corrections
    - condition: observable $\mathcal{O}_{\mathcal{O}(k)}$ must exhibit non-analytic dependence on λ, e.g. event-shape variables, ...

C-parameter: linear power corrections

linear power corrections to C-parameter: **[F. Caola et al, JHEP 12 (2022) 062]**

$$\mathcal{T}_\lambda[I_C] = \frac{15}{128\pi}\frac{s_{12}^3}{1-z_3}\left(\frac{\lambda}{q}\right)\left[\frac{(1+z_3)}{2}K\left(c_{12}^2\right) - (1-z_1z_2)\,E\left(c_{12}^2\right)\right] \tag{23}$$

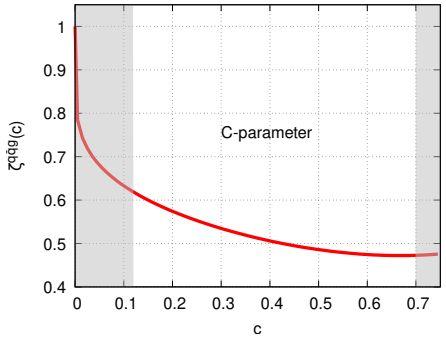

→ find agreement previous with results (2-jet limit, ...)

→ have **analytic** results for entire 3-jet region and these are superior to numerical methods

→ could be used for α_s determinations

[P. Nason, G. Zanderighi, JHEP 06 (2023) 058]

Top quark pair production at the Tevatron: $p_{t\perp}$, y_t, $s_{t\bar{t}}$

- it is now straightforward to compute the linear shift for $p_{t\perp}$, y_t and $s_{t\bar{t}}$

$$\frac{\delta_{\rm NP}\left[p_{t\perp}\right]}{p_{t\perp}} = \frac{\alpha_s}{2\pi}\frac{\pi\lambda}{m_t}\frac{\left(2C_F - C_A\tau\right)}{2\left(1-\tau\right)} \qquad \text{with } \tau = \frac{4m_t^2}{s_{t\bar{t}}} \text{ and } \lambda\alpha_s \sim 0.3 \text{ GeV}$$

$$\delta_{\rm NP}\left[y_t\right] = \frac{\alpha_s}{2\pi}\frac{\pi\lambda}{m_t}\left[\left(3C_A - 8C_F\right)\tau\cosh^2 y_t - \left(C_A - 2C_F\right)\frac{\tau\left(2-\tau\right)}{4\left(1-\tau\right)}\sinh\left(2y_t\right)\right]$$

$$\frac{\delta_{\rm NP}\left[s_{t\bar{t}}\right]}{s_{t\bar{t}}} = \frac{\alpha_s}{2\pi}\frac{\pi\lambda}{m_t}\left[2C_F\left(1-\tau\right) - C_A\,\tau\cosh\left(2y_t\right) + \left(3C_A - 8C_F\right)\sinh\left(2y_t\right)\right]$$

- can now compute non-perturbative shift at Tevatron ($\sqrt{s} = 1.8$ TeV)